HIGH STRAIN MEASUREMENTS DURING FATIGUE CYCLING IN FIBRE REINFORCED THERMOPLASTIC COMPOSITES USING IMBEDDED DRAW TOWER FIBRE BRAGG GRATING SENSORS

Voet E. [1], Luyckx G. [1], De Baere I. [1], Degrieck J. [1], Bartelt H. [2], Vlekken J. [3], Jacobs E. [3]

[1] *Dept. of Mechanical Construction and Production -Labo Soete, Ghent University (UGent), B-9000 Gent, Belgium*
[2] *Institute of Photonic Technology (IPHT), D-07745 Jena, Germany*
[3] *Fibre Optic Sensors & Sensing Systems (FOS&S), B-2440 Geel, Belgium*

ABSTRACT

This paper presents the experimental study of fibre Bragg gratings for measuring strain inside composite laminates during fatigue loading. The optical fibres are embedded inside thermoplastic CFRP test-coupons with an ultimate strain of about 1.1%. Tension – tension fatigue cycling at a rate of 5Hz is been carried out at 314MPa with a maximum strain of 0.51%. At such extreme strain levels the use of high strength sensors becomes inevitable. Neither the sensor nor the composite test-coupons showed any significant degradation even after more than 500000 cycles. Fibre optic Bragg grating sensors are known to be very accurate strain sensors but one should be very careful interpreting their response once they are imbedded inside composite materials. Polarization effects due to induced birefringence and transverse strain effects together with non-uniform strain effects are demonstrated based on observations on the spectral response of the sensor. However, a good correlation was found between the strain measurements of an electrical extensometer and the fibre Bragg grating sensor during the complete cycling. The high strength imbedded sensors show that they are very feasible for extreme and long term strain measurements.

KEYWORDS: fibre reinforced thermoplastic composite, fibre Bragg grating, imbedding, structural health monitoring, birefringence effect

1. INTRODUCTION

High performance carbon fibre reinforced plastics are today more and more employed as structural parts in advanced engineering constructions. As composites are complex materials their real long term behavior is hard to predict. As such it becomes very interesting to use fibre optics for (in-situ) *structural health monitoring (SHM)* and to measure *real-time* the strain and stress of (critical) composite structural parts under load. In the past few years the use of fibre optic sensors based on the *fibre Bragg grating (FBG)* principle has become a very interesting and potential technology for accurate strain measuring purposes. A fibre Bragg grating is highly sensitive to *strain* and *temperature* and shows good *linear response* over a large measurement range. FBG sensors have many advantages and enter into strong competition with electrical strain gauges, mainly because they are small, they have a self referencing capability without electromagnetic interference and because they can easily be multiplexed and imbedded. In literature one can find that FBG sensors are already extensively been imbedded and tested mostly in *'thermoset'* composite materials. They have proven their feasibility for (low) strain measurements and for sensing damage effects in composites [1][2][3]. Within this study '*high strength draw tower fibre Bragg grating sensors*' are imbedded in a CETEX® laminate, which is a high performance *carbon fibre reinforced composite* with a polyphenylenesulphide (PPS) *'thermoplastic'* matrix. Tensile testing was

performed on the composite test-coupons and the *spectral response* of the sensors is investigated during and after cycling in comparison with an externally mounted electrical extensometer. *Polarization tests* are carried out on imbedded sensors in order to gather more information on the *in-situ strain state* of the composite. First experimental results of the behavior of the imbedded high strength fibre Bragg grating sensors are presented.

2. MATERIALS & METHODS

2.1.THERMOPLASTIC COMPOSITE MATERIAL (CETEX®)

The sensors were imbedded in *carbon fibre reinforced (woven fabric) polyphenylenesulphide (PPS)* host material, called *CETEX®* (Ten Cate Advanced Composites, The Netherlands). This thermoplastic composite has excellent mechanical properties (Table 1) and is designed for the aerospace industry. It consists of stacked thin *'semi-preg'* sheets (lamina) of *satin woven fabric* pre-impregnated with *PPS matrix* material, thickness 0.32mm, which are mould together during a *hot press cycle* to form *CFR thermoplastic laminates*. In Table 1 are given the engineering constants of the in-plane properties of the individual lamina:

Table 1 In-plane elastic (left) –and tensile strength properties (right) of the individual carbon/PPS lamina (by dynamic modulus identification method & mechanical testing at TUDelft, respectively).

E_{11} [GPa]	E_{22} [GPa]	ν_{12} [-]	G_{12} [GPa]		X_T [MPa]	ε_{11}^{ult} [-]	Y_T [MPa]	ε_{22}^{ult} [-]	S_T [MPa]
56	57	0.033	4.175		617	0.011	754	0.013	110

More information on fabrication is found in section 3.3 where the imbedding process is shortly explained together with the process to manufacture the test-specimens.

2.2.DRAW TOWER FIBRE BRAGG GRATING TECHNOLOGY

Basic FBG theorem. Fibre optic sensors based on fibre Bragg grating technology are *'wavelength selective reflective filters'* inside the core of an optical fibre with the reflected *Bragg wavelength,* λ_B as *main parameter* (see Fig. 1) :

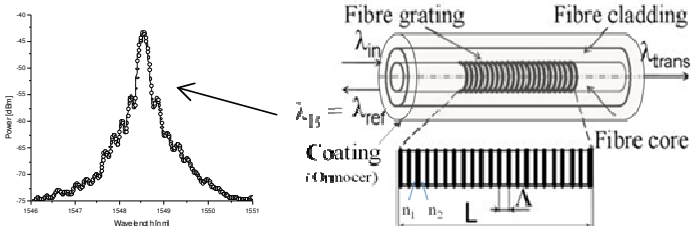

Fig. 1 Representation of a fibre Bragg grating and its reflected Bragg spectrum (left)

An FBG is an area in the core of an optical fibre that has successive zones with alternating refractive index (i.e. n_1, n_2) and effective refractive index n_{eff}. The *basic Bragg condition* is then given by:

$$\lambda_B = 2 \cdot n_{eff} \cdot \Lambda \qquad \text{Eq. 1}$$

The FBG is in principle sensible for two physical parameters: i.e. *strain* and *temperature*. By taking the differential of Eq.1 and deriving for strain as well temperature one yields:

$$\frac{\Delta\lambda}{\lambda} = (1 - P)\Delta\varepsilon + (\alpha_n + \alpha_f)\Delta T \qquad \text{Eq. 2}$$

With *P the strain-optic coefficient* and α_n the *thermo-optic coefficient* and α_f the *thermal expansion coefficient* of the optical fibre. Strain calibrations and experimental data measured for a number of fibre Bragg gratings of the same batch as the ones used in these experiments delivered a *strain-optic coefficient* of approximately *P = 0.22*. This calculated value falls in the range of the values reported in literature [4][5] and will further be employed for strain calculations.
Values for α_n and α_f for GeO_2 doped silica fibres (see next subsection) are 5.9 10^{-6} K^{-1} and 0.55 10^{-6} K^{-1} respectively [6]. The value for α_n is a weighted mean value confirmed by a number of experiments and temperature calibrations. Together with the FBG-wavelength, these coefficients are defined as the *linear strain* and *temperature sensitivities* $s_\varepsilon = (1 - P) \cdot \lambda_B = 0.78$ and $s_T = (\alpha_n + \alpha_f) \cdot \lambda_B = 6.45 \cdot 10^{-6}$. With this the *linear approximation* gets:

$$\Delta\lambda = s_\varepsilon \cdot \Delta\varepsilon + s_T \cdot \Delta T \qquad \text{Eq. 3}$$

With s_ε *and* s_T *the linear sensitivities*, $\Delta\varepsilon$ the difference in *longitudinal strain* and ΔT *the difference in temperature*, both inducing a *Bragg wavelength shift,* $\Delta\lambda$. Typical values for s_ε and s_T for an FBG in the C-band region (1520nm – 1570nm) are *1.2 pm/με and 10 pm/°C*, respectively. It should be noted that these sensitivities are in fact wavelength dependent – they are directly proportional to the FBG-wavelength λ_B - but for small wavelength changes they are normally approximated as being constant. The relative error induced by using the (linear) sensitivities to calculate the strain or temperature are small and are kept below 1%.

Draw Tower fibre Bragg gratings. *High strength draw tower fibre Bragg gratings* (DTGs) are manufactured using one single laser pulse while drawing the fibre, i.e. with the *coating added* directly *after the FBG inscription* [7], as such no re-coating is necessary. These FBGs are written in a (special) single mode optical fibre with core- and cladding-diameter of 6µm and 125µm, respectively. Such an optical fibre is made of *fused Silica* (SiO_2) with a *highly Ge-doped (GeO_2) core* (approx. 18mol%) for *high photosensitivity,* necessary for inscribing the FBG. The imbedded fibre draw tower gratings used in these experiments have a length of L_{FBG} *= 4mm* and an outer diameter, with surrounding *ORMOCER coating* (ORganic MOdified CERamic) of approx. 195µm. The coating material provides *excellent mechanical properties* such as a *tensile strain* value between *5-6%.*

3. EXPERIMENTS & FIRST RESULTS

3.3.IMBEDDING PROCESS

Carbon fibre reinforced PPS plates, CETEX®, with $[(0°,90°)]_{2s}$ stacking sequence are fabricated by piling *four 'semi-preg' layers* and pressing it together with appropriate pressure and temperature. *Optical fibres* are put *in between* two layers of *semi-preg* (completely impregnated with PPS polymer) and can be fixated in orientation by using an Ultrasonic welding device and a small piece of PPS-sheet. *Test-coupons* are sawn and prepared with composite tabs as shown in Fig. 2:

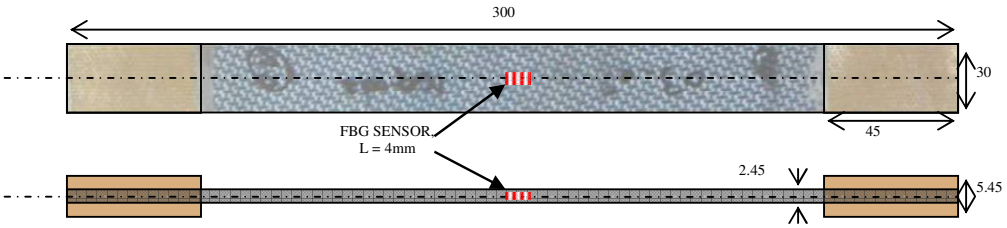

Fig. 2 Representation of a composite test-coupon with imbedded fibre Bragg grating sensor

During the *hot press cycle* the sensors have to withstand *extreme temperature* and *pressure* for a couple of hours, exceeding 300°C and 10bar, respectively. The draw tower fibre Bragg grating sensors are imbedded in the centre of symmetric stacked CETEX® test-coupons, see Fig. 2:
The sensors together with their protective coating *survived* the process and are found feasible for imbedding in CETEX® material. An example of the *spectral response* is shown in Fig. 3:

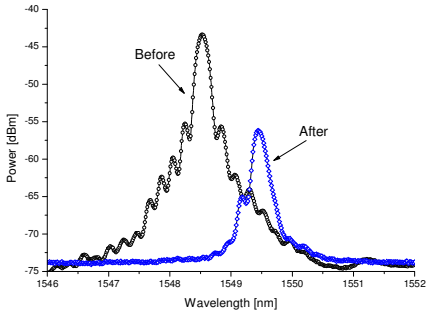

Fig. 3 Bragg spectrum before and after imbedding

After the imbedding process the Bragg peak encounters a *high loss in reflected power* (approx. 15dB) which is a combination of *three effects*: At first, optical power is mostly lost by *bending of the fibre* due to the fibre-outcome *at the edge* of the laminate, because of some outflow and curing of the PPS matrix. Secondly, power is attenuated due to the *woven fabric structure* as the optical fibre is squeezed in between two layers during fabrication (i.e. *microbending*). However, this contribution is small in comparison with the first effect. Finally, a *non-uniform strain distribution* over the length of the fibre grating is induced by the woven fabric *together* with a *birefringence effect* induced in the core of the fibre by the high *shrinkage* of the *matrix* material. These latter effects are translated into a distortion of the *spectrum* (i.e. *peakwidth increases and total peakpower decreases*).
The spectral behavior of imbedded sensors is further analyzed together with *polarization testing* (see Section 3.5), as such more information on the *internal strain distribution* is gathered.

3.4.TENSION – TENSION FATIGUE TESTING

Tensile testing was carried out at a mechanical test-bench INSTRON 8081 which was *automated* to correlate *optical* measuring data and the *mechanical parameters* of the INSTRON equipment. An *electrical extensometer* was mounted on the surface of the test coupon *at the position of the DTG*. The test-coupons with imbedded sensors are then submitted to *tension-tension fatigue cycling* at 314MPa and a frequency of 5Hz for

more than 500000 cycles. In total *14 sequences* of *40200cycles* were carried out. This was *alternated* with *quasi-static testing* carried out in 23 incremental steps of 1kN (approx. 13.7MPa/step) till max. 23kN (approx. 314MPa) and back. At each step the *load* was held *constant* for about *60sec* to process the *data* of the *FBG sensor*, the *extensometer* and the *load cell* at the same time. The *imbedded sensors* show a *very good response* to the *applied stress* and a pretty good correlation between the strain and stress measurements can be reported during the complete cycling, as shown in Fig. 4 and Fig. 5:

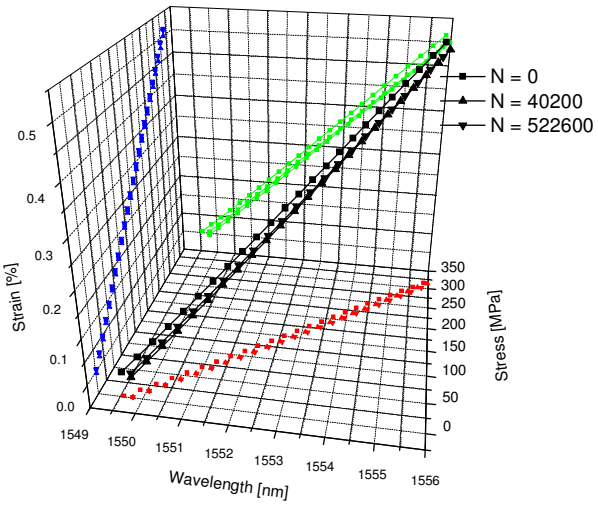

Fig. 4 XYZ-plot representing the three registered parameters during quasi-static testing and its interdependence (i.e. Wavelength vs Strain vs Stress) during quasi-static testing at *N = 0, 40200 and 522600* cycles

A *clear linear dependence* is found between the parameters even after more than 500000 cycles. However, taking a closer look at the measurements of the quasi-static testing one notices there is a slight *difference* found between the *response* of the *imbedded strain sensor* and the strain measurements of the *surface mounted extensometer*, see linear curves in Fig. 5:

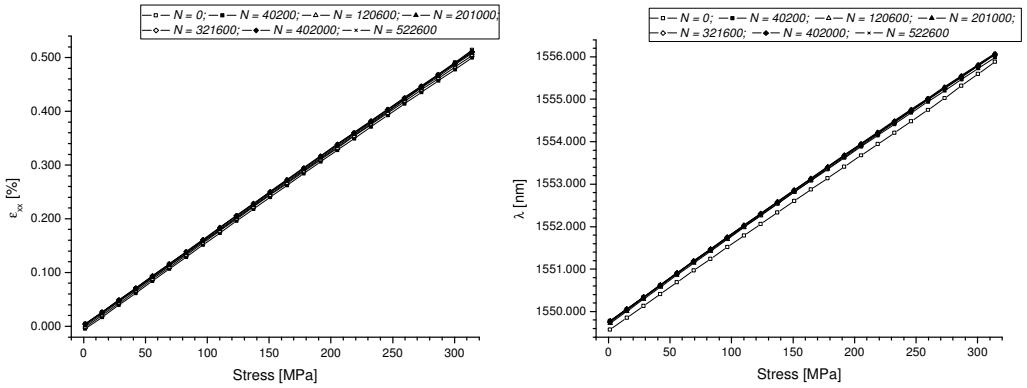

Fig. 5 *Strain* extensometer (left) and *wavelength shift* DTG (right) vs. *Stress* applied on the test coupon plotted for 7 sequences

The *DTG sensor* shows an *increase* in *wavelength* after the first cycling which indicates a *plastic deformation* (i.e. *settlement of the sample*). From Fig. 5 it is difficult to notice any effect of the extensometer. A *summary* of the results of seven sequences is *plotted*

in Fig. 6 where the minimum, maximum and mean values of both sensors (i.e. extensometer on the left y-axis and DTG on the right y-axis) illustrate there is a *difference in response*. The exact values are found in Table 2 and Table 3, with in the latter also added the mean values of the temperature FBG located next to the sample in order to monitor environmental temperature fluctuations. The DTG sensor shows a mean wavelength shift of +154pm or a positive shift in strain of 0.0127% but the extensometer on the other hand shows a compression of 0.0118% relative to the values at the start of sequence 1 (see dashed and dotted lines in Fig. 6). This is however explained by *slippage* of the *extensometer knifes* that occurred during cycling between the first and the second sequence.

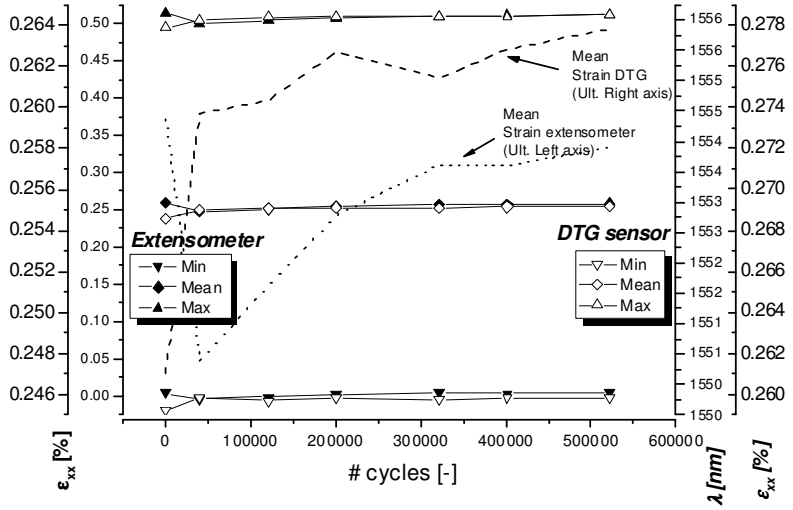

Fig. 6 Minimum, mean and maximum plotted at seven sequences (from 0 till 522600 cycles) for extensometer (left y-axis) and imbedded DTG sensor (right y-axis)

After further cycling both sensors respond very similar at maximum stress levels but they behave quite different at minimum levels. By *converting* wavelength shifts *into strain* and comparing the values with the ones obtained from the extensometer (Table 2), one notices the *imbedded sensor* measured consequently *higher strain values* (again slippage of the extensometer during cycling is a plausible explanation).

Table 2 Minimum and maximum values at seven sequences

		Minimum Values (left y-axis)			**Maximum Values (right y-axis)**		
Sequence	# cycles	Strain Extensometer	Wavelength DTG	Strain DTG	Strain Extensometer	Wavelength DTG	Strain DTG
[-]	[-]	[%]	[nm]	[%]	[%]	[nm]	[%]
1	0	0.00462	1549.573	0	0.51422	1555.882	0.52198
2	40200	-0.00428	1549.777	0.01686	0.49952	1555.986	0.53058
4	120600	-0.00126	1549.728	0.01282	0.50381	1556.049	0.53582
6	201000	0.00176	1549.775	0.01674	0.50773	1556.060	0.53668
9	321600	0.00457	1549.750	0.01462	0.50983	1556.054	0.53624
11	402000	0.00355	1549.773	0.01655	0.51071	1556.065	0.53713
14	522600	0.00472	1549.776	0.01681	0.51144	1556.085	0.53881

It should be noted that the strain values of the *imbedded sensor lean very close against theoretical obtained values* when calculating with (e.g. $\sigma_{max,th}$=314Mpa, $\varepsilon_{max,th}$=0.55%). Also the *response* of the DTG at maximum loading shows a (slight) *constant increase* in strain after *each sequence*; indicating small plastic deformation of the test-coupon (i.e. *settlement* of the woven fabric) during cycling. This clearly shows the *imbedded sensor* kept *good bonding* with the composite, even after 500000 cycles. The measurements of the *extensometer* show *more spreading*, however after sequence 9 both sensors react very similar at maximum applied stress. This indicated that measuring strain on the surface or inside the laminate are two completely different approaches and one should be *careful correlating* both measurements.

Table 3 Mean values at seven sequences, plotted on ultimate left and right y-axis in Fig. 6

		Mean Values Strain		**Mean Values Wavelength**	***Mean Values Wavel. Temp***
Sequence	# cycles	*Ult. Left y-axis* Extensometer	*Ult. Right y-axis* DTG	*Right y-axis* DTG	*Temperature FBG*
[-]	[-]	[%]	[%]	[nm]	*[nm]*
1	0	0.25942	0.26099	1552.727	*1549.825*
2	40200	0.24762	0.27372	1552.881	*1549.838*
4	120600	0.25127	0.27432	1552.888	*1549.834*
6	201000	0.25475	0.27671	1552.917	*1549.827*
9	321600	0.25720	0.27543	1552.902	*1549.834*
11	402000	0.25713	0.27684	1552.919	*1549.835*
14	522600	0.25808	0.27781	1552.931	*1549.837*

3.5.FBG SENSOR RESPONSE

Non-uniform strain effects and induced birefringence. In order to gather *more information* of the *spectral behavior* we carried out a more detailed *analysis* of the *spectrum* during quasi-static loading. As an example, *two different test-samples* (cut out of the same composite plate) are studied. Both test-coupons have one DTG imbedded (with $\lambda_{NOM}\approx$ 1549nm & L_{FBG}=4mm); however at first sight both sensors show a different response. An example of the spectral response is shown in Fig. 7 at *two different stress levels*. One notices the peak of the FBG at the right manifests a clear *peak separation*; indicating a *birefringence effect* inside the core of the optical fibre, induced by a small *difference* in *transversal strain* inside the grating.

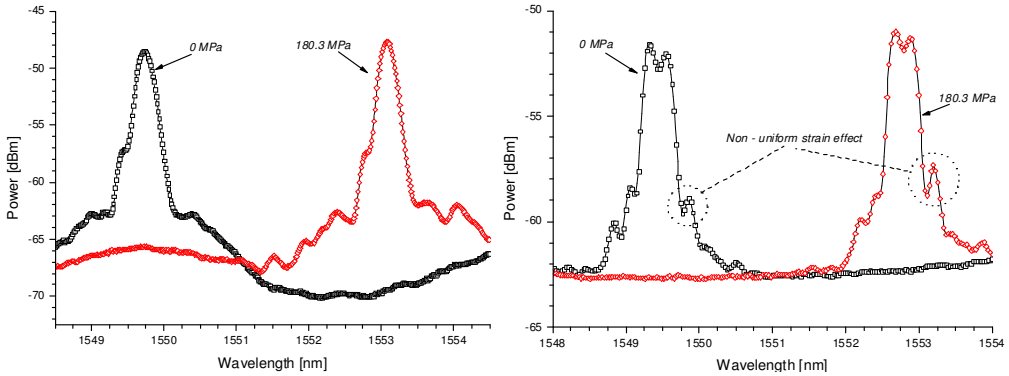

Fig. 7 Spectral response of two imbedded DTG sensors during quasi-static testing at two different stress levels

This *residual strain effect* is induced *during composite fabrication* and is actually a *combination* of pressure applied during *hot pressing* (molding) and *shrinkage of the PPS* polymer. Because of variation of the (surrounding) structure over the length of the DTG sensor (i.e. woven carbon fabric and matrix material) *non-uniform strain* effects and *induced birefringence* are present *at the same time* when loading the sample (see Fig. 7). Because it is *not* always *easy* to *distinguish* both *effects,* a *detailed analysis* of the spectra is necessary. An example of a *non-uniform strain* effect together with the *induced birefringence* is clearly shown in the spectra in Fig. 7 at the right. This effect is not immediately visible in the spectra shown at the left, although both sensors are imbedded in the same composite plate. However, both sensors are imbedded in different test-coupons, they are not positioned (locally) at exactly the same spot in between the semi-preg layers; as such, another response is quite possible.

Polarization analysis. Extensive polarization measurements, using a HP polarization controller to adapt the *linear polarization* angle of the light coupled in the core of the optical fibre, yielded a better insight of the *strain-optic effects* inside both imbedded FBGs, see Fig. 8 and Fig. 9:

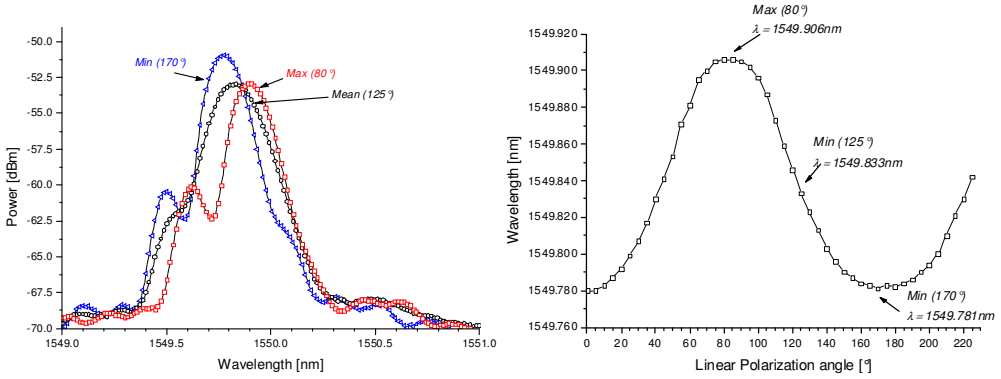

Fig. 8 Spectra from *sensor 1* taken at different polarization angles showing the min., mean and max. spectrum (Left), and the respective peak wavelengths (determined with Centre of Gravity, COG method) for the complete angular rotation (Right)

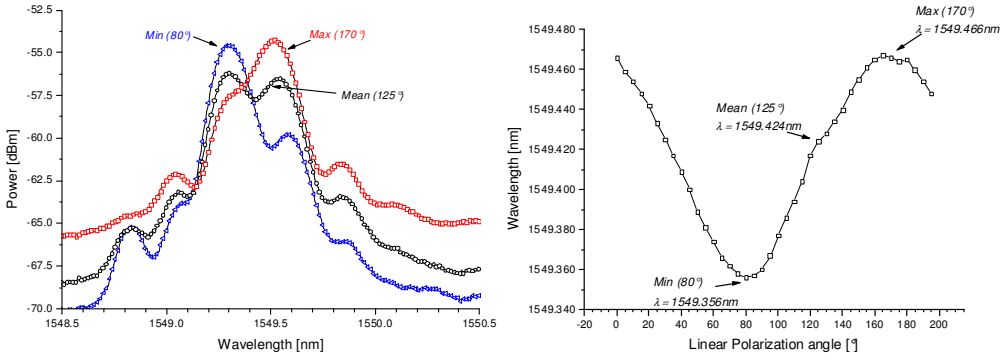

Fig. 9 Spectra from *sensor 2* taken at different polarization angles showing the min., mean and max. spectrum (Left), and the respective peak wavelengths (determined with Centre of Gravity, COG method) for the complete angular rotation (Right)

With the polarization controller we are able to rotate the linear polarization angle of the light which is coupled into the optical fibre. This polarized light was rotated for more

than 180° in steps of 5°. At each angle a spectrum of the Bragg peak was taken and each time the peak wavelength was determined using a 'Centre Of Gravity method' (COG) (see right plot in Fig. 8 & Fig. 9). As such, it is possible to determine the *degree* of *birefringence*, which is directly *proportional* to the *transverse strains* induced in the *core* of the optical fibre [8]. *Peak separation* of the Bragg peak for a single mode optical fibre is given as:

$$\frac{\Delta\lambda_{max}-\Delta\lambda_{min}}{\lambda_{B,nom}} = \frac{\Delta\lambda_{tot}}{\lambda_{B,nom}} = \frac{n_{eff}^2}{2}(p_{12}-p_{11})(\varepsilon_y-\varepsilon_x) \qquad \text{Eq. 4}$$

Using the COG data calculated at each linear pol. angle and using Eq. 3 it is possible to determine the difference in transversal strain, i.e. $(\varepsilon_y - \varepsilon_x)$. One should notice it is actually not possible to determine the individual transverse strains ε_x and ε_y with single axial FBGs, due to the isotropic nature of the single mode optical fibre, and thus *only* a *difference* in *transverse strain* can be calculated from these polarization measurements.
For example from Fig. 8 & Fig. 9 both sensors show a difference in wavelength between the minimum –and maximum peak of approx. 0.125nm and 0.110nm, respectively. This means, although there is no clear peak separation visible from Fig. 8, both sensors sense a difference in transverse strain in the same order of magnitude. Using Eq. 3 with $\Delta\lambda_{tot}$ = 0.120nm, $\lambda_{B,nom}$ = 1549nm, n_{eff} = 1.456, p_{11}=0.113 and p_{12}=0.252 one can calculate a *residual strain, (ε_y - ε_x) of approx. 0.053%.*
These polarization measurements indicate that the sensors are capable of measuring differences in residual -and transverse strain. However, it should be noted no exact peak wavelength values are obtained, as by using the COG method one has to define manually a threshold value in order to cut the Bragg peak at a certain level (e.g. at -3dB) and eventually to process the wavelength difference between the separated peaks. As within the spectral response both effects are represented (i.e. non-uniform axial strain along the grating and induced birefringence) *not very accurate COG values* are obtained from the individual spectra and *transverse effects are at a rough estimate*. Also coating issues should be included when interpreting the sensor' response, as there is always a str*ain transfer* from composite material to the sensing element. This strain transfer is dependent on the type of loading and is of course influenced by the coating properties of the sensor. For axial loading of composite samples this transfer can be approximated as being 100%, but for transversal strain the transfer coefficient can decrease down to 60% or less, meaning that the actual birefringence sensed by the DTG is in reality induced by a transverse stress that is 1.67 times higher in magnitude. These values can be estimated by detailed FEM simulations and will be considered in future analysis.
In order to look at *changes* in *transverse strain during loading* of the test-coupons, the same *polarization tests* as shown in Fig. 8 and Fig. 9 were performed *during quasi-static testing* till a maximum tension of $\sigma_{max}\approx$180MPa. However, wavelength difference obtained from the peak separation at *zero loading* and at *maximum loading* showed *no significant changes* in *birefringence*. This actually points out that *Poisson effects* inside the test-specimen are *very small* in x- and y-direction when performing tension testing and thus that *no significant* influence on the spectrum is found during loading. As such one can *neglect* transverse *effects* during fatigue loading and can assume that *axial strain* measurements of the DTG sensors during fatigue cycling (as shown in Section 3.4) are *quite accurate*.

4. CONCLUSIONS

This paper reported the use of imbedded *high strength DTG sensors* for monitoring *extreme strain (>0.5%)* during fatigue cycling of *thermoplastic CFRP test-coupons*. The sensors *survived* well the *hot-press fabrication cycle* although some attention should be payed to reduce loss during and after imbedding. The fibre optic sensor showed a *quite good response* to the *applied stress* over the complete cycling even after *more than 500000 cycles*. Some *different response* is reported between the *surface mounted extensometer* and the *imbedded sensor* which is mostly explained by settlement of the extensometer' knifes during cycling. *Polarization measurements* were performed in order to estimate the *induced birefringence* effect in the optical fibre and thus the difference in *transverse strain* can be obtained from the *spectral response* of the imbedded DTG.

Further analyses on the level of the imbedded sensor and its coating is necessary and will be carried out in the next in order to verify the *accuracy of the measurements*, to *define* more in detail *polarization effects* and *transverse strain* inside the core of the optical fibre and eventually to *determine the "real" in-situ strain state* of the composite.

REFERENCES

[1] De Waele W, Degrieck J, Baets R, Moerman W, and Taerwe L, Load and deformation monitoring of composite pressure vessels by means of optical fibre sensors: *Insight* 43(8), 2001, pp518-525

[2] E Bocherens, S Bourasseau, V Dewynter-Marty, S Py,M Dupont, Ferdinand and H Berenger†Damage detection in a randome sandwich material with embedded fiber optic sensors, Smart Materials and Structures, 2000, 9 310–315

[3] Seiji Kojima, Shinji Komatsuzaki, Yoshinori Kurosawa, Akihito Hongo, Embedding type strain sensors using small-diameter fiber Bragg grating to composite laminate structures, HITACHI CABLE REVIEW No.23, AUGUST 2004

[4] Rao, Y.-J., In-fibre Bragg grating sensors: Meas. Sci. Technol., 1997, 8:355-375

[5] A. Othonos, K. Kalli: Fiber Bragg Gratings, Artech House, 1999, ISBN 0-89006-344-3

[6] V.J. Hagemann, Untersuchungen zum dynamischen Einzelpuls-Einschreiben von Faser-Bragg-Gittern un zu deren Anwendung, PhD, 2001

[7] C. Chojetzki, M. Rothhardt, H.-R. Müller, H. Bartelt, Large Fibre Bragg Grating Arrays for monitoring applications – Made by Drawing Tower Inscription, IPHT, Jena, Germany & FOS&S, Geel, Belgium, 2005.

[8] F. Bosia, P. Giaccari, J. Botsis, M. Facchini, H. G. Limberger & R. P. Salathé, Characterization of the response of fibre Bragg grating sensors subjected to a two-dimensional strain field, Smart Materials and Structures 12, 2003, 925-934.